



# Investigation into heat transfer and fluid flow characteristics of liquid two-layer and emulsion in microwave processing☆



Waraporn Klinbun<sup>a</sup>, Phadungsak Rattanadecho<sup>b</sup>

<sup>a</sup> Faculty of Engineering and Technology, PANYAPIWAT Institute of Management, Nonthaburi 11120, Thailand

<sup>b</sup> Center of Excellence in Electromagnetic Energy Utilization in Engineering (CEE), Thammasat University (Rangsit Campus), Khlong Luang, Prathum Thani, 12121 Thailand

## ARTICLE INFO

Available online 17 December 2015

### Keywords:

Emulsion  
Microwave  
Rectangular waveguide  
Temperature profile

## ABSTRACT

Numerical study of fluid flow and heat transfer within two types of liquid (liquid two-layer and oil–water emulsion) when subjected to microwave energy are discussed. In order to obtain the simulation of microwave heating from room temperature, a 2D comprehensive model was integrated with electromagnetic field, incompressible laminar flow and heat transfer. The effects of layered configuration, layered thickness and dispersed fraction of emulsions were investigated. Temporal profiles obtained using fiber optic sensors at four discrete points were compared with the simulated temperature profiles. The simulated outlet temperatures of liquid had a good agreement with experimental data within the maximum prediction error of 5%. The theory presented in this paper can be effectively used to explain fluid transport during microwave heating system using the rectangular waveguide.

© 2015 Elsevier Ltd. All rights reserved.

## 1. Introduction

The major advantages of microwave heating are rapid and volumetric heating. Microwave can penetrate the surface and produce volumetric heat generation within materials, thus leading to high energy efficiency and short process time. However, non-uniform heating is a disadvantage of microwave heating. The complex interaction of microwaves with sample properties produces non-uniform heating. A particular microwave oven can behave differently for the same sample depending on its physical state such as liquid two-layer and emulsion. This non-uniform heating in a microwave oven not only affects food safety but also influences food quality [1].

Most of the work on microwave heating system design and processes has been done based on only experience and perception of engineers. In addition, experimental study alone is quite difficult to gain the reasons behind non-uniform heating in a microwave oven. A modeling technique is powerful tool can provide a complete platform to study the effects of microwave oven design and food properties on non-uniform heating. Coupled electromagnetic and multi-physics (momentum and heat) equations can describe microwave heating and would help in design microwave ovens and optimize process parameters to minimize non-uniformity issues [2].

Refer to the literature, there were many the theoretical studies on combined microwave and thermal transport [3–20]. The various kinds

of dielectric materials are chosen to illustrate microwave heating phenomena.

For liquid sample, Zhang et al. [9] proposed a 3D mathematical model for the heating of water and oil layer with time dependent dielectric properties in microwave cavity. Zhu et al. [16] presented the numerical modeling of continuous flow microwave heating of liquids layer. The results revealed that the heating pattern strongly depends on the dielectric properties of liquids and geometry of the microwave system. Cha-um et al. [19] studied heating process of liquids using microwave with a rectangular waveguide numerically and experimentally. The effects of sample sizes, placement of sample inside the guide, and microwave power were considered in detail. The numerical results agreed well with experimental data. Salvi et al. [21] developed model to simulate temperature profiles in Newtonian and non-Newtonian fluids for continuous flow microwave heating by COMSOL Multiphysics. Recently, Yousefi et al. [22] investigated on microwave heating of flowing water in ANSYS Multiphysics. Various factors were examined; namely, the effects of inlet velocity, applicator height and applicator diameter on the temperature field. A 2D numerical model using COMSOL was developed by Choi et al. [23]. It was to validate uniform heating of particulate foods in a continuous flow microwave and ohmic combination heater. The developed model was included with an electric field, electromagnetic field, incompressible laminar flow, forced-coupling method, heat transfer and arbitrary Lagrangian–Eulerian (ALE) moving mesh technique. The simulated outlet temperature of particulate foods was compared with experimental data. The maximum prediction error was 4%.

For layered sample, Rattanadecho [24] investigated the thawing of layered sample using microwave oven. It is shown that, the variation of layered configurations and layer thickness affected to thawing rate

☆ Communicated by W.J. Minkowycz.

E-mail addresses: [warapornkli@pim.ac.th](mailto:warapornkli@pim.ac.th) (W. Klinbun), [ratphadu@enr.tu.ac.th](mailto:ratphadu@enr.tu.ac.th) (P. Rattanadecho).

**Nomenclature**

$A$	area ( $\text{m}^2$ )
$C_p$	specific heat capacity ( $\text{J}/(\text{kg K})$ )
$E$	electric fields intensity ( $\text{V}/\text{m}$ )
$f$	frequency of incident wave ( $\text{Hz}$ )
$g$	gravitational constant ( $\text{m}/\text{s}^2$ )
$h_c$	local heat transfer coefficient ( $\text{W}/\text{m}^2\text{K}$ )
$H$	magnetic field intensity ( $\text{A}/\text{m}$ )
$k$	thermal conductivity ( $\text{W}/\text{mK}$ )
$L_x$	width of the rectangular waveguide ( $\text{m}$ )
$P$	power ( $\text{W}$ )
$p$	pressure ( $\text{Pa}$ )
$Q$	local electromagnetic heat generation term ( $\text{W}/\text{m}^3$ )
$T$	temperature ( $^\circ\text{C}$ )
$t$	time ( $\text{s}$ )
$\tan \delta$	dielectric loss coefficient ( $-$ )
$u, w$	velocity component ( $\text{m}/\text{s}$ )
$Z_H$	wave impedance ( $\Omega$ )
$Z_l$	intrinsic impedance ( $\Omega$ )

**Greek letters**

$\varphi$	volume fraction of dispersed phase ( $-$ )
$\alpha$	thermal diffusivity ( $\text{m}^2/\text{s}$ )
$\beta$	coefficient of thermal expansion ( $1/\text{K}$ )
$\eta$	dynamic viscosity ( $\text{Pa}\cdot\text{s}$ )
$\varepsilon$	permittivity ( $\text{F}/\text{m}$ )
$\lambda$	wavelength ( $\text{m}$ )
$\mu$	magnetic permeability ( $\text{H}/\text{m}$ )
$v$	velocity of propagation ( $\text{m}/\text{s}$ )
$\nu$	kinematics viscosity ( $\text{m}^2/\text{s}$ )
$\rho$	density ( $\text{kg}/\text{m}^3$ )
$\sigma$	electric conductivity ( $\text{S}/\text{m}$ )
$\omega$	angular frequency ( $\text{rad}/\text{s}$ )
$\xi$	surface tension ( $\text{N}/\text{m}$ )

**Subscripts**

$0$	free space
$\infty$	ambient condition
$c$	continuous phase
$d$	dispersed phase
$eff$	effective
$r$	relative
$in$	input
$x, y, z$	axis

due to its dielectric properties of phase change materials during microwave thawing process. Promas et al. [25] concerned with the energy and exergy analyses in the drying process of non-hygroscopic porous packed bed using a combined multi-feed microwave-convective air and continuous belt (CMCB). The results showed that using the CMCB had the several advantages over the conventional method. Klinbun and Rattanadecho [20] studied numerically the heating of multilayer porous packed bed which subjected to microwave power. This study aimed to understand effects of layered configuration, layered thickness and operating frequency. The results were presented in electric field distribution, heat transfer and velocity flow.

The layered liquids and emulsions are the common food systems, such as milk, salad dressing, mayonnaise, sauces, and many more [18]. Therefore, understanding the influences of various parameters during microwave processing of layered liquid and emulsions are required because of the wide usage of microwave systems.

The most emulsions are considered as oil-in-water (o/w) and water-in-oil (w/o). An earlier investigation on microwave heating of

multiphase system and emulsions was reported by Barringer et al. [26]. They studied experimentally for various oil–water fractions and layered system with fixed beaker radii in a household microwave oven. They found the dielectric properties and sample size determined in which sample resonant absorption occurred. Chan and Chen [27], Rajaković and Skala [28], and Nour et al. [29] carried out experimental studies on the conditions of demulsification of water-in-oil emulsions by microwave technology. After that, Samanta and Basak [18] carried out the preliminary theoretical analysis on efficient microwave processing of 1D oil–water emulsion (o/w and w/o) placed on ceramic plates (alumina, SiC). The results were shown that an alumina support at the left side may be recommended as the optimal heating strategy for both o/w and w/o emulsion samples whereas SiC support may be favored for o/w emulsion sample due to lesser thermal runaway. In addition, microwave energy was applied to separate or demulsify of emulsions. For example, Palou et al. [30] studied the demulsification of an o/w emulsion prepared with Mexican heavy crude oil. A comparative study was carried out between microwave and oil bath heating with regard to water separation time. From the results, microwave dielectric heating used less time than conventional oil bath heating. Water separation of O/W emulsions increased with microwave power and salt content of the aqueous phase, and in the presence of a chemical demulsifier. Binner et al. [31] was investigated the separation of water-in-oil emulsions using natural gravity settling and microwave heating techniques. The result was found that the thermal effect of microwave heating leads to improvements in settling times.

Due to the large amount of past studies are primarily considered on microwave heating of pure substance or layered system. There are a few works which investigate of microwave processing of multiphase system, especially emulsions. Therefore, the various parameters are still not fully understood and a number of critical issues still remain unsolved. The characteristics of microwave heating of emulsions and layered materials are very complicated, thus the study in more detail should be systemically studied.

This research was to develop a comprehensive fully coupled multi-physics model that includes heat and momentum transfer in model liquid system. In this article, the simulated results were compared with experimental heating profiles of a model. The effects of layered configuration, layered thickness, dispersed phase fraction, and dielectric properties of emulsion are studied. The results presented here provide a basis for fundamental understanding of microwave heating of layered liquid and oil–water emulsions.

**2. Experimental study****2.1. Sample preparation**

The two-layer and emulsion of oil–water were studied. The oil-in-water emulsion, designated as o/w emulsion and water-in-oil emulsion, designated as w/o emulsions. In case of two-layer is considered in two models: w-o bed (water layer on oil layer), and o-w bed (oil layer on water layer). The sample size is chosen to be  $109.22 \times 54.61 \times 50$  mm.

**2.2. Apparatus**

Fig. 1 shows the experimental apparatus for microwave heating using a rectangular waveguide system. It was a monochromatic wave of  $\text{TE}_{10}$  mode operating at a frequency of 2.45 GHz. The magnetron (Micro Denshi Co., model UM-1500) generated microwave energy that was transmitted along the z-direction of the rectangular waveguide with inside dimensions of  $110 \times 55$  mm toward a water load that was situated at the end of the guide. The water load ensured that only a minimal amount of microwave was reflected back to the sample. An isolator on the upstream side of sample is used to trap microwave was reflected from the sample in order to prevent the microwave from damaging the magnetron. The sample heated was liquid layer of 50 mm in thickness,

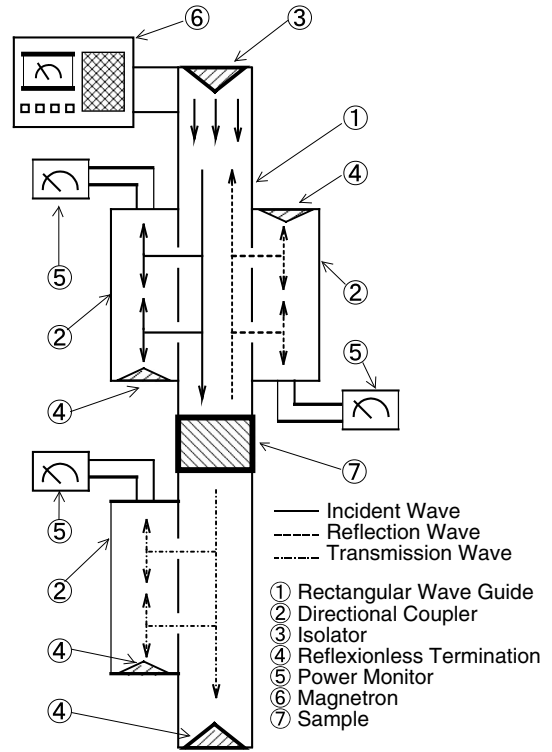


Fig. 1. Experimental apparatus for microwave heating system; (a) equipment setup and (b) microwave measuring system [19].

which is filled in container with a thickness of 0.75 mm and is made from polypropylene. During the experiment, output of magnetron was set at 500 W. The powers of incident, reflected and transmitted waves were measured by a wattmeter using a directional coupler (Micro Denshi Co., model DR-5000). The temperature was measured with a Luxtron fluoro optic thermometer model 790 (accurate to  $\pm 0.5$  °C) which were placed in the center of the sample at each 10 mm interval.

### 3. Mathematical modeling

The model was developed to predict heat and fluid flow during heating by microwave energy. The Maxwell's equations of electromagnetic were solved to obtain the electric field inside the cavity and sample and coupled with a multi-physics model to obtain a temperature and velocity distribution in 2D in Fig. 2.

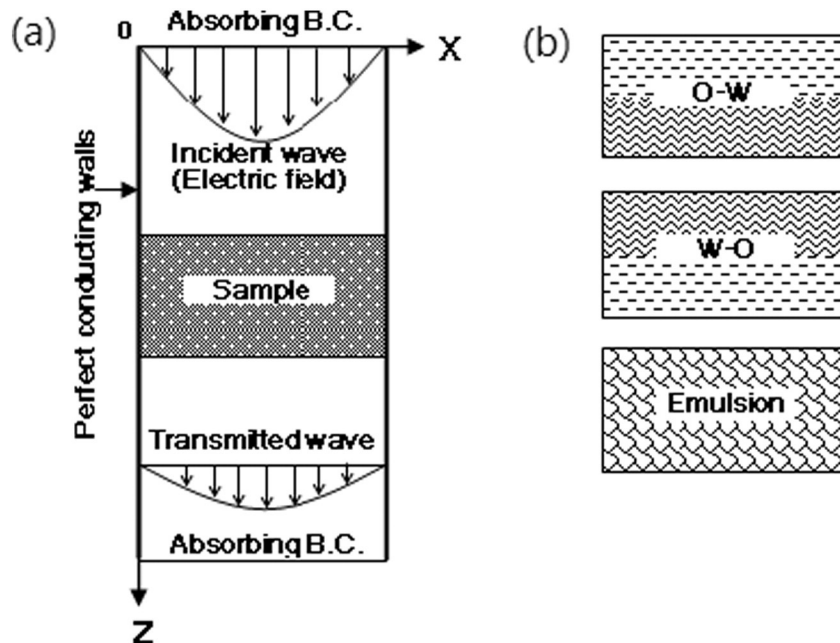


Fig. 2. Physical model; (a) computational domain and (b) sample [20].

### 3.1. Electromagnetic model

In this work, electromagnetic wave was considered in the TE<sub>10</sub> mode which does not change in the direction between the broad faces. The Maxwell's equations for electromagnetic wave in TE<sub>10</sub> mode can be written as [19]:

$$\frac{\partial E_y}{\partial z} = \mu \frac{\partial H_x}{\partial t} \quad (1)$$

$$\frac{\partial E_y}{\partial x} = -\mu \frac{\partial H_z}{\partial t} \quad (2)$$

$$-\left(\frac{\partial H_z}{\partial x} - \frac{\partial H_x}{\partial z}\right) = \sigma E_y + \varepsilon \frac{\partial E_y}{\partial t} \quad (3)$$

where permittivity or dielectric constant  $\varepsilon$ , magnetic permeability  $\mu$  and electric conductivity  $\sigma$  are defined by:

$$\varepsilon = \varepsilon_0 \varepsilon_r, \mu = \mu_0 \mu_r, \sigma = 2\pi f \varepsilon \tan \delta \quad (4)$$

The dielectric properties are a function of volume fraction and temperature, as follow:

$$\varepsilon_r(\varphi, T) = \varepsilon'_r(\varphi, T) - j\varepsilon''_r(\varphi, T) \quad (5)$$

For water [10]:

$$\varepsilon'_r(T) = 85.56 - 0.3099T - 2.328 \times 10^{-3}T^2 + 4.107 \times 10^{-5}T^3 - 1.728 \times 10^{-7}T^4 \quad (6)$$

$$\tan \delta(T) = 0.2314 - 6.405 \times 10^{-3}T + 9.37 \times 10^{-5}T^2 - 7.415 \times 10^{-7}T^3 + 2.415 \times 10^{-9}T^4 \quad (7)$$

For corn oil [9]:

$$\varepsilon'_r(T) = 2.587 + 0.001313T + 3.998 \times 10^{-6}T^2 \quad (8)$$

$$\varepsilon''_r(T) = 0.1214 + 0.00172T + 1.454 \times 10^{-6}T^2 \quad (9)$$

For o/w emulsions [18]:

$$\varepsilon_r = \frac{\varepsilon_{rc}[\varepsilon_{rd}(1+a\varphi) + a\varepsilon_{rc}(1-\varphi)]}{\varepsilon_{rd}(1-\varphi) + \varepsilon_{rc}(a+\varphi)} \quad (10)$$

For w/o emulsions [18]:

$$\ln \varepsilon_r = \varphi \ln \varepsilon_{rd} + (1-\varphi) \ln \varepsilon_{rc} \quad (11)$$

Power absorbed per unit volume from the microwaves at any location of the sample was calculated from the electric field distribution inside the sample:

$$Q = 2\pi f \cdot \varepsilon_0 \cdot \varepsilon'_r(\tan \delta)(E_y)^2 \quad (12)$$

**Boundary conditions:** The walls of the rectangular cavity were assumed to be perfect electric conductors and hence the tangential component of the electric field was set to zero.

$$H_n = 0, E_t = 0 \quad (13)$$

At the both ends of cavity was absorbing condition by Mur [32]:

$$\frac{\partial E_y}{\partial t} = \pm v \frac{\partial E_y}{\partial z} \quad (14)$$

The microwave source is simulated by the equations [10]:

$$E_y = E_{yin} \sin\left(\frac{\pi x}{L_x}\right) \sin(2\pi f t) \quad (15)$$

$$H_x = \frac{E_{yin}}{Z_H} \sin\left(\frac{\pi x}{L_x}\right) \sin(2\pi f t) \quad (16)$$

where  $f$  is the frequency of microwave,  $L_x$  is the width of the incidence plane,  $Z_H$  is the wave impedance, and  $E_{yin}$  is the input value of the electric field intensity. By applying the Poynting theorem, the input value of the electric field intensity is evaluated by the microwave power input as:

$$E_{yin} = \sqrt{\frac{4Z_H P_{in}}{A}} \quad (17)$$

where  $P_{in}$  is the microwave power input and  $A$  is the area of the incident plane.

### 3.2. Heat transfer and fluid flow model

A 2D multi-physics model was formulated to describe the momentum and heat transfer inside the sample. The two samples included in the liquid model were water and corn oil. The energy conservation equation was solved for the mixture and the effect of microwave heating was included as a source term obtained from the electromagnetic model. For momentum balance, the Boussinesq approximation takes into account of the effect of density variation on the buoyancy force.

**Continuity equation:**

$$\frac{\partial u}{\partial x} + \frac{\partial w}{\partial z} = 0 \quad (18)$$

**Momentum equations:**

$$\frac{\partial u}{\partial t} + \left(u \frac{\partial u}{\partial x} + w \frac{\partial u}{\partial z}\right) = -\frac{1}{\rho} \left(\frac{\partial p}{\partial x}\right) + \nu \left(\frac{\partial^2 u}{\partial x^2} + \frac{\partial^2 u}{\partial z^2}\right) \quad (19)$$

$$\frac{\partial w}{\partial t} + \left(u \frac{\partial w}{\partial x} + w \frac{\partial w}{\partial z}\right) = -\frac{1}{\rho} \left(\frac{\partial p}{\partial z}\right) + \nu \left(\frac{\partial^2 w}{\partial x^2} + \frac{\partial^2 w}{\partial z^2}\right) + g\beta(T-T_\infty) \quad (20)$$

**Energy equation:**

$$(\rho C_p)_{eff} \frac{\partial T}{\partial t} + (\rho C_p)_{eff} \left(u \frac{\partial T}{\partial x} + w \frac{\partial T}{\partial z}\right) = k_{eff} \left(\frac{\partial^2 T}{\partial x^2} + \frac{\partial^2 T}{\partial z^2}\right) + Q \quad (21)$$

where

$$(\rho C_p)_{eff} = (1-\varphi)(\rho C_p)_c + \varphi(\rho C_p)_d \quad (22)$$

$$k_{eff} = (1-\varphi)k_c + \varphi k_d \quad (23)$$

where the suffixes 'c' and 'd' represent the continuous and dispersed phases, respectively.

**Boundary conditions:** Only the top surface of the sample was open for energy transfer and the other surfaces were insulated. In addition, the Marangoni flow [10] was incorporated as a boundary condition. Finally, the initial temperature of sample is 28 °C.

$$-k \frac{\partial T}{\partial z} = h_c(T-T_\infty) \quad (24)$$

$$\eta \frac{\partial u}{\partial z} = -\frac{d\xi}{dT} \frac{\partial T}{\partial x} \quad (25)$$

where  $k$ ,  $h_c$  are thermal conductivity and heat transfer coefficient, respectively.  $\eta$  is dynamic viscosity and  $\xi$  is surface tension

### 3.3. Input parameter

Dielectric properties of the samples as function of temperature and volume fraction and thermal properties (heat capacity, thermal conductivity and coefficient of thermal expansion) were obtained from literatures. The detail was showed in Table 1.

### 3.4. Numerical solution

The electromagnetic and the multi-physics model were fully coupled as the dielectric properties of the sample, which were obtained from literature, were a function of temperature and volume fraction. The coupling procedure was showed in Fig. 3. The Maxwell's equations (Eqs. (1)–(3)) are solved using the finite difference time domain (FDTD) method with boundary conditions given by Eqs. (13)–(16). To ensure stability of the time-stepping algorithm  $\Delta t$  is chosen to satisfy the courant stability condition:

$$\Delta t \leq \frac{\sqrt{(\Delta x)^2 + (\Delta z)^2}}{c} \quad (26)$$

And the spatial resolution of each cell defines as:

$$\Delta x, \Delta z \leq \frac{\lambda_g}{10\sqrt{\epsilon_r}} \quad (27)$$

In this work, a time step of  $\Delta t = 2 \times 10^{-12}$  s is used to solve Maxwell's equations. The grid size is  $\Delta x = 1.0922$  mm and  $\Delta z = 1.0$  mm.

For the sample, energy and momentum equations were solved using a cell centered finite control volume along with the SIMPLE algorithm developed by Patankar [33]. The time step is 0.01 s. The fully implicit time discretization finite difference scheme is used to arrive at the solution in time. The each time step iterations are continued until the relative error is less than  $10^{-6}$  (error  $\leq 10^{-6}$ ).

## 4. Results and discussion

### 4.1. Characterizing electric field distribution

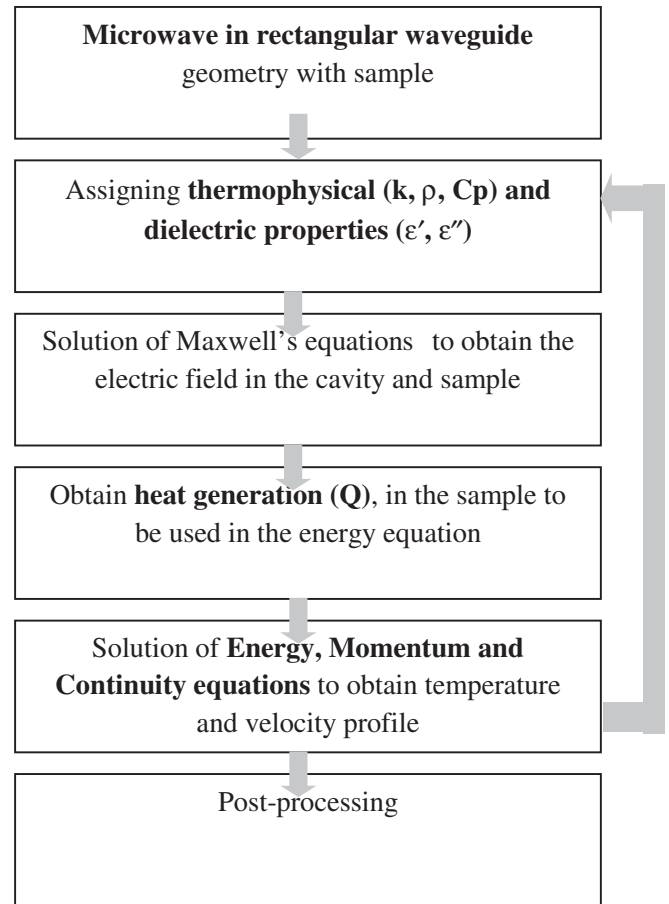
Because the first objective is to understand the change in electric field density during heating of two-layer and emulsion at various dielectric properties, the coupled models were used to determine the electric field power density within the liquid sample. The electric field distribution inside the cavity and sample was showed in Fig. 4.

Fig. 4 presents the simulation of the typical electric field of TE<sub>10</sub> mode along the center axis ( $x = 54.61$  mm) of rectangular waveguide. The vertical axis represents the intensity of the electric field  $E_y$ , which is normalized to the amplitude of the input electromagnetic wave,  $E_{yin}$ .

In Fig. 4(a) and (b), corresponding to that cases of single layer liquid, since the microwave passing through waveguide having low permittivity is directly irradiated to the sample having high permittivity, large part of microwaves are reflected from the surface of the sample and interfered with forward wave propagated from the wave input region

**Table 1**  
Thermal property for computational model.

Properties	Air	Water	Corn oil
$\rho$ (kg m <sup>-3</sup> )	1.205	1000	920
$C_p$ (J kg <sup>-1</sup> K <sup>-1</sup> )	1007	4186	2100
$k$ (W m <sup>-1</sup> K <sup>-1</sup> )	0.0257	0.61	0.17
$\eta$ (kg (ms) <sup>-1</sup> )	$1.983 \times 10^{-5}$	$1.793 \times 10^{-3}$	$6.072 \times 10^{-3}$
$\beta$ (K <sup>-1</sup> )	$3.43 \times 10^{-3}$	$5.344 \times 10^{-4}$	$3.8 \times 10^{-4}$



**Fig. 3.** Algorithm for coupling of electromagnetism and heat transfer and fluid flow.

cause a stronger standing wave with large amplitude is formed within cavity. However, the electric field within the sample is almost extinguished where the electric field attenuated owing to microwave energy absorbed, and thereafter the microwave energy absorbed is converted to the thermal energy. In addition, reflected wave from water layer surface are much higher than that of an oil layer due to permittivity of oil layer is higher than air not so much, the small part of microwave is reflected from the surface of oil layer.

Fig. 4(c) shows the distribution of electric field for the cases of 2o-2w layers. The large part of microwaves can penetrate into the sample; the wave reflected from the lower surface has the same order as propagating wave. The large amplitude and wavelength is formed inside the sample by contribution of propagating and reflected waves, such pattern can lead to higher microwave energy absorbed in the interior in comparison with other cases. Fig. 4(d) shows the distribution of electric field for the cases of 2w-2o layers. It can be observed that the distribution of electric field for this case is nearly the same as that water layer (Fig. 4(b)). Therefore, the presence of water layer at the incident floor slightly affects the distribution of electric field because the major parts of microwaves are reflected from the surface.

By comparing Fig. 4(e) and (f), the small part of microwave is reflected from the surface of 1o-3w. Therefore, the oil layer at thickness of 12.5 mm (1o-3w) strongly affects the distribution of electric field due to large part of microwave can penetrate through the surface.

Fig. 4(g) and (h) were similar; it is observed that electric field within emulsions sample is slightly decreased along the depth of sample. It is also interesting to observe that the electric field intensity for the case of 75% o/w sample is greater than the electric field intensity for the case of 25% o/w emulsions. This is because the higher oil content in the emulsions results in smaller effective dielectric loss and higher

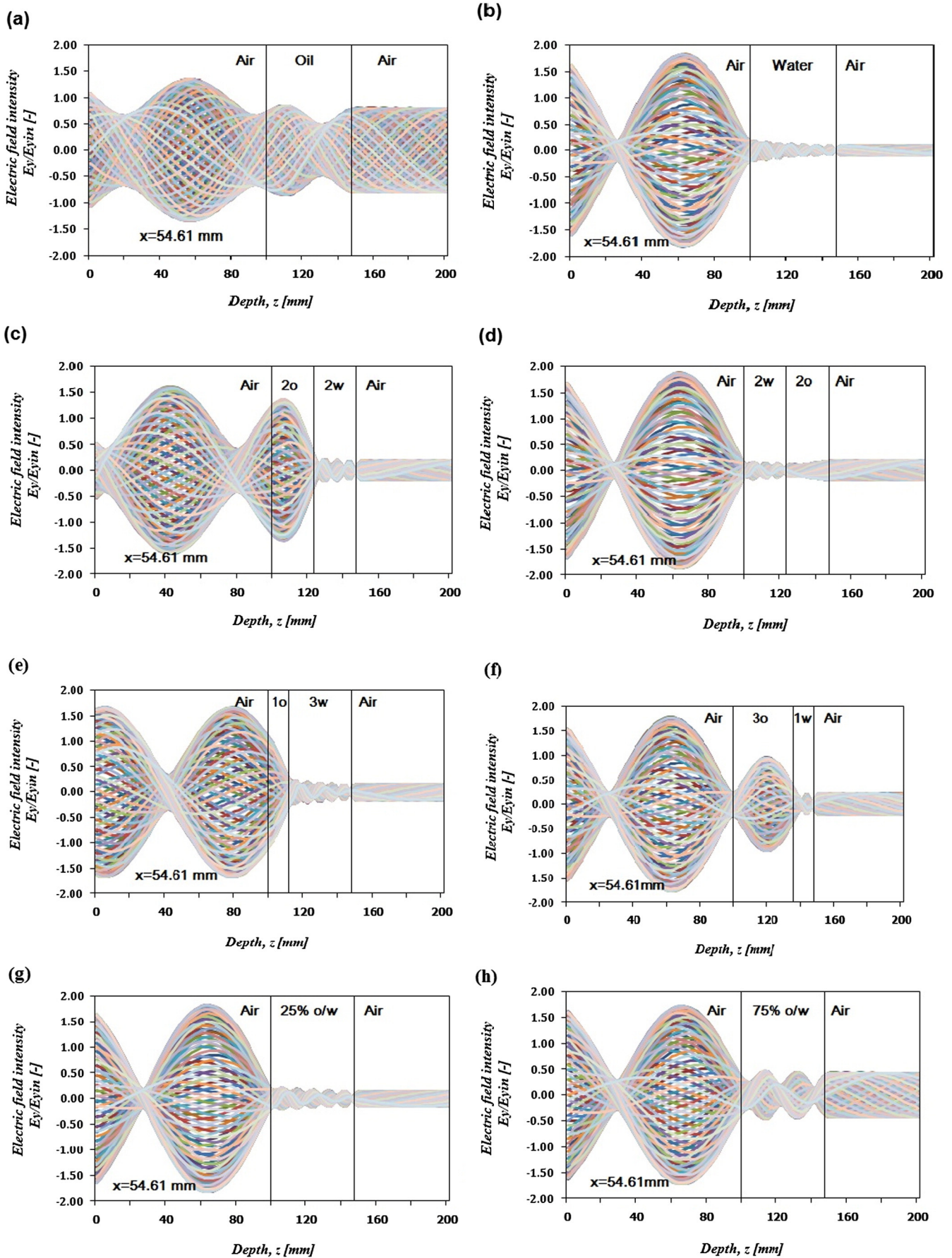


Fig. 4. Electric field distribution inside cavity and sample ( $P = 500$  W,  $f = 2.45$  GHz,  $t = 60$  s).

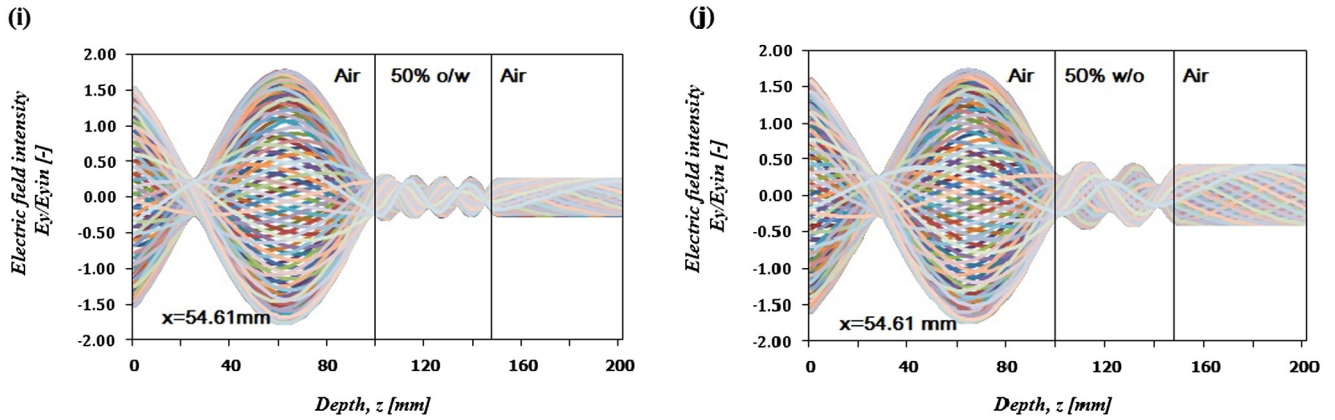


Fig. 4 (continued).

penetration depth. Therefore, emulsions with higher oil contents would show the higher electric field intensity.

Fig. 4(i) and (j) was shown that the electric field is depended on the continuous phase of emulsions (o/w or w/o) and an amplitude of electric field for the case of w/o emulsions is found to be higher than that for the case of o/w emulsions.

#### 4.2. Time-temperature profile

Temporal profiles obtained using fiber optic sensors at four discrete points were compared with the simulated temporal profiles. Fig. 5 compared the observed and simulated temperatures during the heating process. Fig. 5(a) showed that temperatures increase with processing time. The comparisons along the horizontal axis ( $x = 55 \text{ mm}$ ) was displayed in Fig. 5(b). It was observed that the temperatures decrease along the depth of sample due to its penetration depth effect. From the comparison between the simulated results and experimental data, it was found that it was agree well for all cases of samples and the difference lie below  $5^\circ\text{C}$ . The small discrepancies maybe resulted from keeping constant of some thermal properties during simulation process. In addition, the uncertainty in temperature measurement might come from the error in measured microwave power input where the calculated uncertainty associated with temperature was less than 2%. From this result, it was clear that model can be used as a real tool for investigating in detail this particular microwave heating of dielectric materials at a fundamental level.

#### 4.3. Spatial temperature profile

Fig. 6 depicts simulation of temperature distribution within liquid sample with heating time of 60 s. The results show the greatest temperature in the upper region (this region close to the incoming microwave) of heating sample with the temperature decreasing toward the lower wall. It is found that the temperature contour agree well with distribution of electric field.

By comparing in each layered configurations, it is seen that the temperature field within sample in case of 2o–2w is significantly greater than that of other cases. The high temperatures occur in the center of heating layers with temperature decreasing toward the side walls of the liquid layer corresponding to the characteristic of  $TE_{10}$  mode. However, the temperatures increase again near the side walls, which is due to the walls being insulated and low rate of heat loss. The distribution of temperature field near the middle region of liquid layer tends to be uniformed, because the strong effect of Marangoni flow causes the hot spot to move from the middle region to the side walls of the container. The surface of liquid layer, that is close to the incoming microwave, heats up to a higher level at a faster rate than anywhere within the liquid layer. Nevertheless, the temperature decreases slowly along the propagation direction because the penetration depth effect.

In case of effect of layered thickness, it was found that the distribution of temperature in the sample is wavy behavior corresponding to that of electric field. In case of the oil layer with thickness of 25.0 mm,

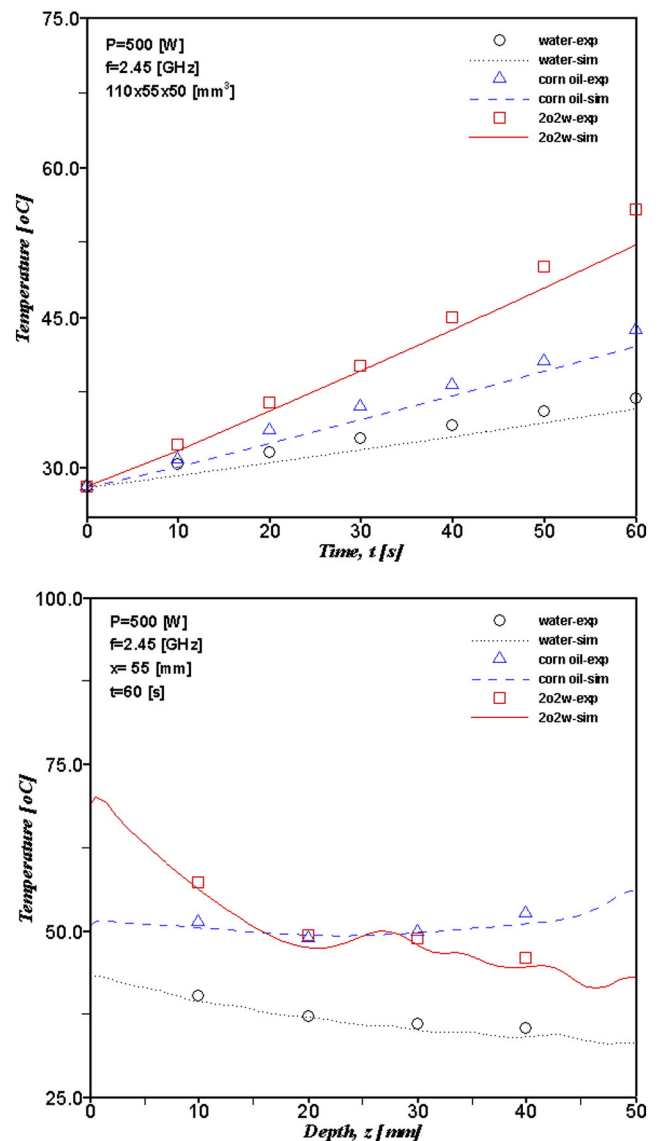


Fig. 5. Simulated and observed time-temperature profile at four locations of sample subjected at 2.45 GHz: (a) during process time and (b) along depth,  $z$  [mm].

the distribution of temperature is higher than the cases with oil layer thickness of 12.5 mm and 37.5 mm. It reveals that a stronger standing wave with large amplitude will be formed within the sample with the optimum oil layer thickness. Thus, a higher maximum temperature will be produced. In addition, the temperature contour in the vertical plane (x-z) for the case of 1o-3w and 3o-1w are illustrated the greatest temperature at upper of heating sample where the microwave is incident.

For effect of dispersed phase fraction, the temperature distributions qualitatively follow the electric field intensity within the emulsions. The greater temperature is observed for the case of 75% oil in water emulsions. This is because of the concentration of dispersed phased increased, the number of interfaces, and thus interfacial reflections increased as results in increase power absorption and consequently heating rate [26]. The two maxima in temperatures occur at the center and near the walls of the rectangular waveguide for all cases of oil in water emulsions due to high electric field intensity of TE<sub>10</sub> mode and the accumulated of heat, respectively. Since the higher microwave power incident at the surface of sample, the maxima in temperature occur at the surface. However, it is found that the maximum temperature occurs at the bottom for the case of 75% o/w sample because the standing waves are formed at the interface between bottom surface and air.

Finally, the comparison of temperature distribution within emulsions between 50% o/w and 50% w/o, it may also be noted that, the greater temperature occurs in the case of o/w emulsions than that the case of w/o emulsions for all directions. The average temperatures within o/w emulsions are 41.62 and 44.89 °C along width, x [mm] and depth, z [mm], respectively whereas average temperatures within w/o emulsions are 38.57 and 41.40 °C along width, x [mm] and depth, z [mm], respectively. The temperature contour for the case of o/w emulsions is higher than that for the case of w/o emulsions.

4.4. Velocity field profile

Fig. 7 illustrated the velocity field within liquid layer and emulsion. The local heating on the surface of liquid layer causes the difference of the surface tension on the surface of liquid layer, which leads to the convective flow of liquid (as Marangoni flow). The liquid flows from the hotter region (higher power absorbed) at the middle of liquid layer to the cold region (lower power absorbed) at the side walls of the container.

By comparing Fig. 7(a) and (b), it is observed that the effect of convective flow in case of water layer becomes stronger than that of oil layer. In Fig. 7(c) and (d), it is seen that the velocity fields are clearly different for each layers.

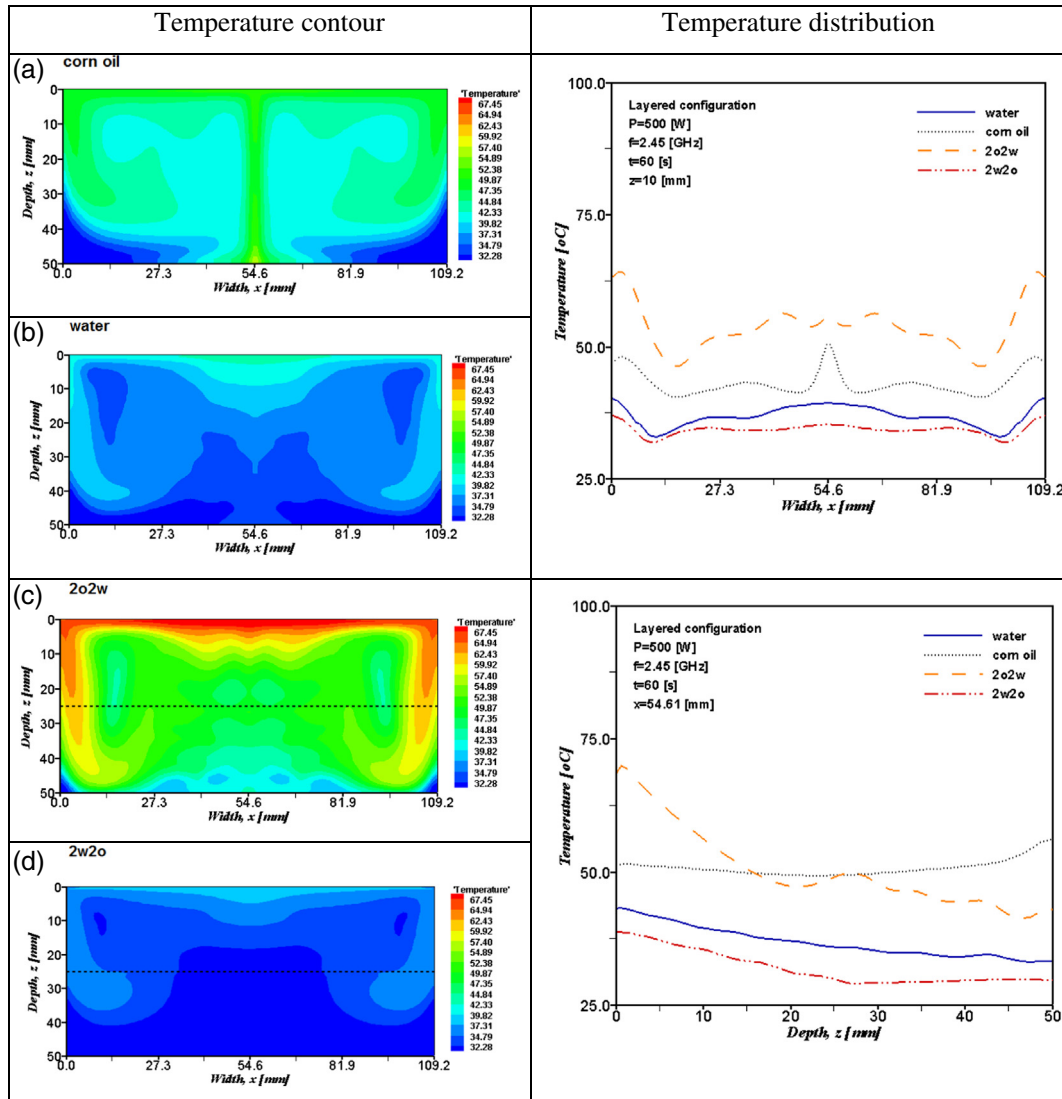


Fig. 6. Spatial temperature profile of the sample due to microwave irradiations (P = 500 W, f = 2.45 GHz, t = 60 s).

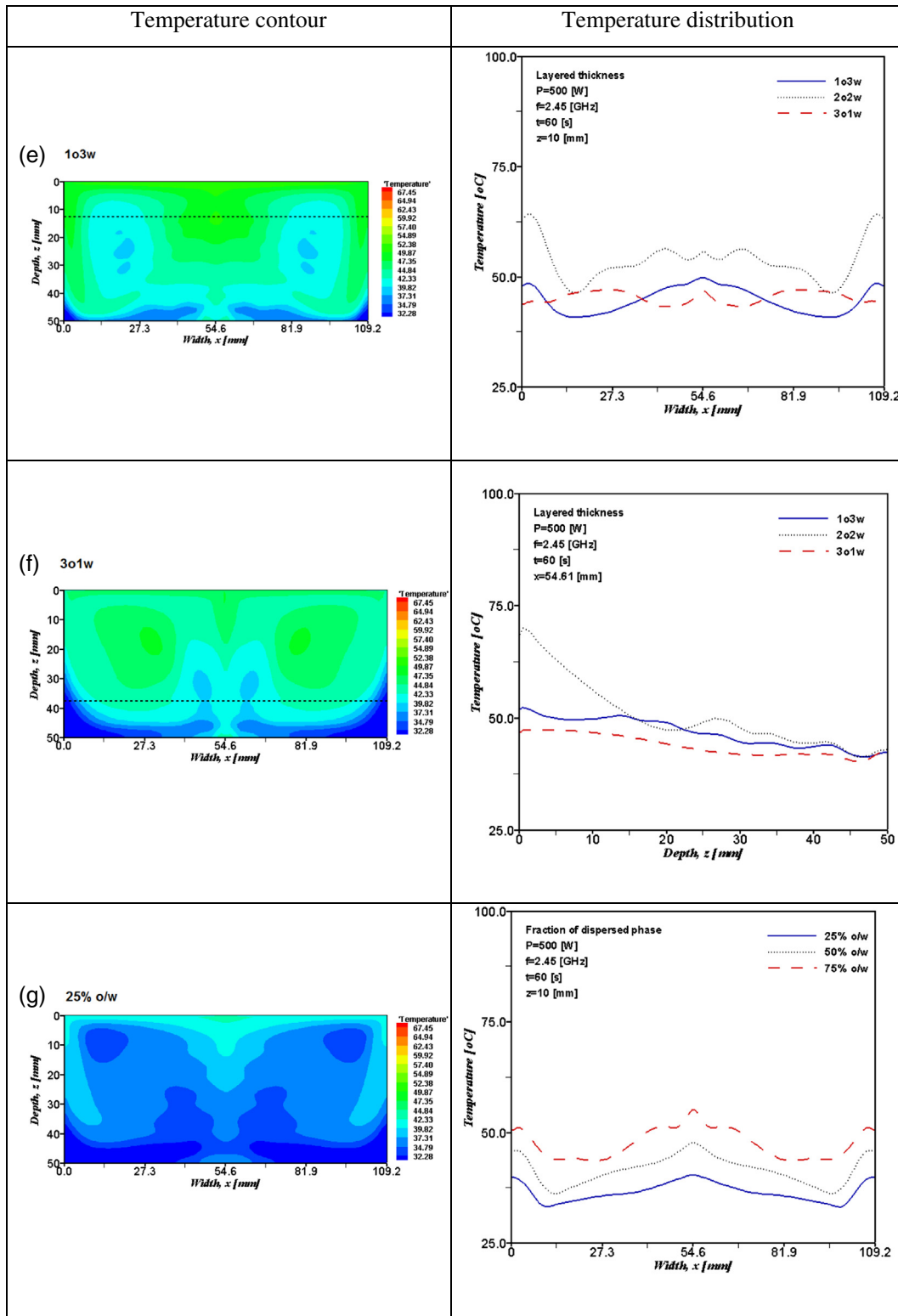


Fig. 6 (continued).

From Fig. 7(e) and (f), the velocity fields are related with the temperature contours for microwave heating of two-layered liquid with various layered thicknesses using a rectangular waveguide. It also observed that the flow patterns in case of 1o-3w and 3o-1w are similar to the single layer of water and oil, respectively because the effect of volume of sample in each layer. The sample with higher oil

content leads to higher penetration depth and stronger resonance of standing wave.

Fig. 7(g) and (h) displayed the flow patterns in vertical plane (x-z) for the case of 25% o/w and 75% o/w, respectively. The velocity fields qualitatively follow the temperature contour. The velocity field is strongly depended on oil fraction ( $\phi$ ) in o/w emulsions.

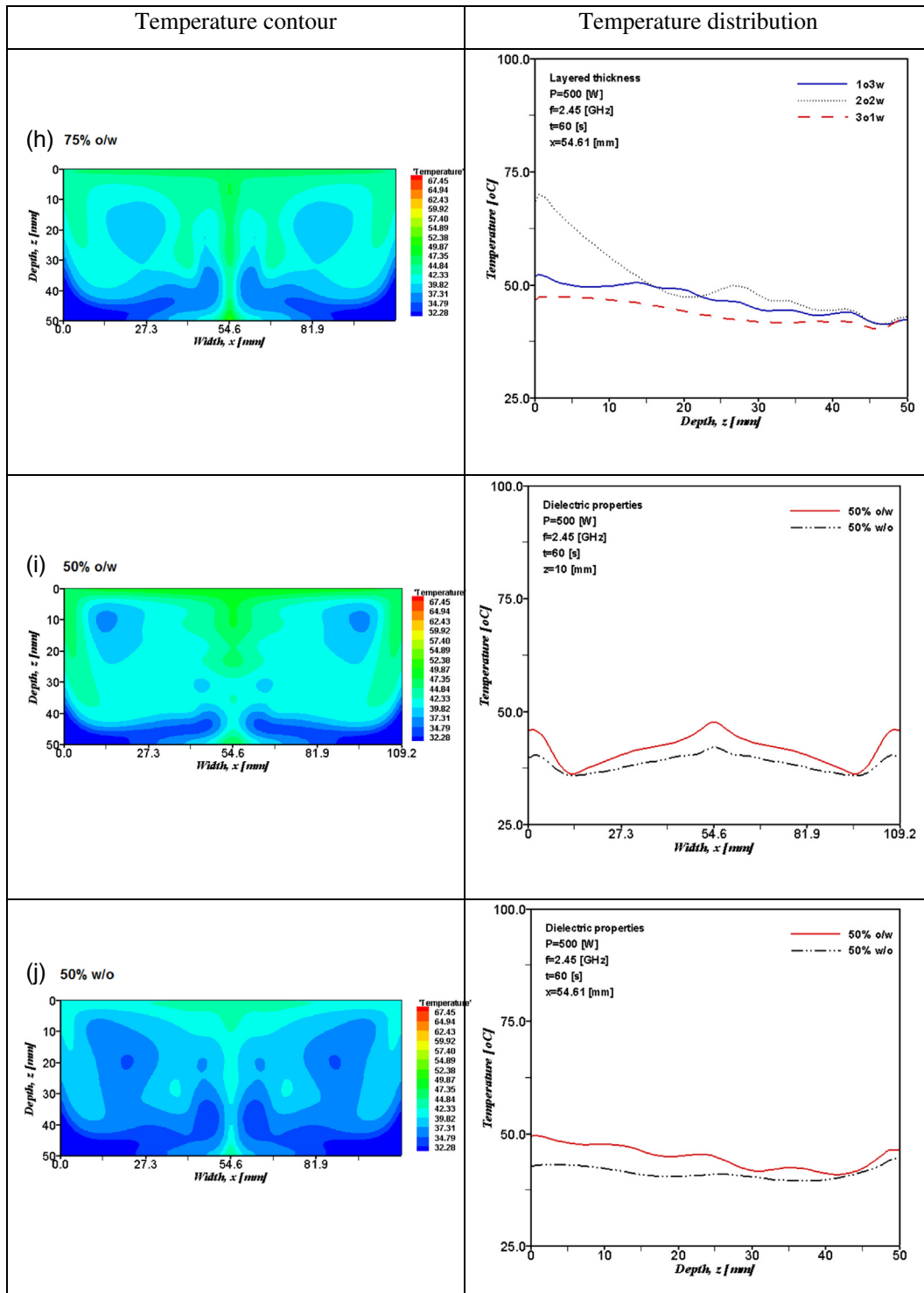


Fig. 6 (continued).

Finally, it was also observed that, the flow pattern (Fig. 7(i)) was similar to Fig. 7(j) but the magnitudes of velocity are different. The key parameters affecting to the fluid flow pattern have been already explained in the first subsection.

**5. Conclusions**

A comprehensive coupled electromagnetic and heat transfer model was developed to simulate microwave heating in rectangular cavity. The simulation results are validated with experimental data at

2.45 GHz. Effects of layered configuration, layered thickness, dispersed fraction, and dielectric properties were studied.

The conclusions of this work can be concluded as followings:

- (1) The presenting model of microwave heating of two-layered liquid and emulsions by using a rectangular waveguide (TE<sub>10</sub> mode) can successfully explain the heating phenomena under various conditions.
- (2) The layered configuration of liquid layers has significant affect to heating pattern and velocity field.

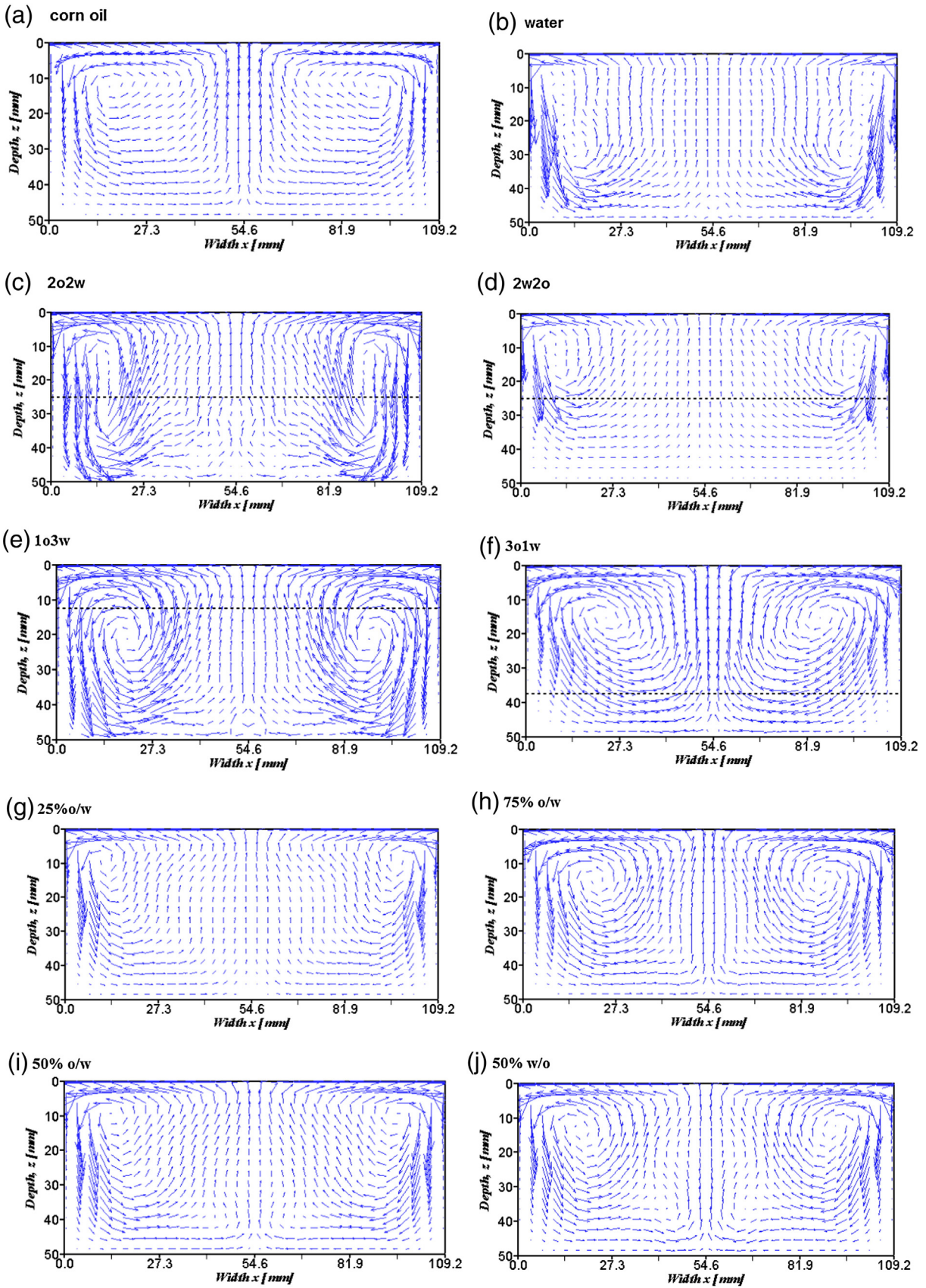


Fig. 7. Spatial velocity profile of the sample due to microwave irradiations ( $P = 500 \text{ W}$ ,  $f = 2.45 \text{ GHz}$ ,  $t = 60 \text{ s}$ ).

- (3) The optimum layered thickness of layered system and the higher oil content of o/w emulsion result in the higher temperature, which is related to the increasing microwave power absorbed.
- (4) The continuous medium of an emulsion has strongly effect on heating pattern.

The next steps of this work highlight the other materials as Emulsions in Porous Media.

### Acknowledgment

The authors gratefully acknowledge the financial support for this work provided by the Thailand Research Fund (under the TRF contract No. RTA5680007) and the Nation Research University Project of Thailand Office of Higher Education Commission.

### References

- [1] L. Ma, D. Paul, N. Potheary, C. Railton, J. Bows, L. Barratt, J. Mullin, D. Simons, Experimental validation of a combined electromagnetic and thermal FDTD model of a microwave heating process, *IEEE Trans. Microwave Theory Tech.* 47 (1995).
- [2] H. Chen, J. Tang, F. Lui, Simulation model for moving food packages in microwave heating processes using conformal FDTD method, *J. Food Eng.* 88 (3) (2008) 294–305.
- [3] A. Metaxas, R. Meridith, *Industrial Microwave Heating*, Peter Peregrinus Ltd, London, 1983.
- [4] H. Prosetya, A. Datta, Batch microwave heating of liquids: an experiment study, *J. Microwave Power Energy* 26 (4) (1991) 215–226.
- [5] K. Ayappa, H. Davis, E. Davis, J. Gordon, Two-dimensional finite element analysis of microwave heating, *AIChE J.* 38 (10) (1992) 1577–1592.
- [6] K. Ayappa, H. Davis, G. Crapiste, E. Davis, J. Gordon, Microwave heating: an evaluation of power formulations, *Chem. Eng. Sci.* 46 (4) (1991) 1005–1016.
- [7] K. Ayappa, S. Brandon, J. Derby, H. Davis, E. Davis, Microwave driven convection in a square cavity, *AIChE J.* 40 (7) (1994) 1268–1272.
- [8] H. Ni, A. Datta, K. Torrance, Moisture transport in intensive microwave heating of biomaterials: a multiphase porous media model, *Int. J. Heat Mass Transfer* 42 (8) (1999) 1501–1512.
- [9] Q. Zhang, T. Jackson, A. Urgan, Numerical modeling of microwave induced natural convection, *Int. J. Heat Mass Transfer* 43 (2000) 2141–2154.
- [10] P. Rattanadecho, K. Aoki, M. Akahori, A numerical and experimental investigation of the modeling of microwave heating for liquid layers using a rectangular wave guide (effects of natural convection and dielectric properties), *Appl. Math. Model.* 26 (3) (2002) 449–472.
- [11] D. Dincov, K. Parrott, K. Pericleous, Heat and mass transfer in two phase porous materials under intensive microwave heating, *J. Food Eng.* 65 (3) (2004) 403–412.
- [12] P. Salagnac, P. Glouannec, D. Lecharpentier, Numerical modeling of heat and mass transfer in porous medium during combined hot air, infrared and microwave drying, *Int. J. Heat Mass Transfer* 47 (2004) 4479–4489.
- [13] V. Romano, F. Marra, U. Tammaro, Modelling of microwave heating of foodstuff: study on the influence of sample dimensions with a FEM approach, *J. Food Eng.* 71 (3) (2005) 233–241.
- [14] V. Vegh, I. Turner, A hybrid technique for computing the power distribution generated in a lossy medium during microwave heating, *J. Comput. Appl. Math.* 197 (1) (2006) 122–140.
- [15] S. Chatterjee, T. Basak, S. Das, Microwave driven convection in a rotating cylindrical cavity: numerical study, *J. Food Eng.* 79 (4) (2007) 1269–1279.
- [16] J. Zhu, A. Kuznetsov, K. Sandeep, Mathematical modeling of continuous flow microwave heating of liquids (effects of dielectric properties and design parameters), *Int. J. Therm. Sci.* 46 (2007) 328–341.
- [17] S. Greedipalli, V. Rakesh, A. Datta, Modeling the heating uniforming contributed by a rotating turntable in microwave ovens, *J. Food Eng.* 82 (2007) 359–368.
- [18] S. Samanta, T. Basak, Theoretical analysis of efficient microwave processing oil-water emulsions attached with various ceramic plates, *Food Res. Int.* 41 (2008) 386–403.
- [19] W. Cha-um, P. Rattanadecho, W. Pakdee, Experimental and numerical analysis of microwave heating of water and oil using a rectangular wave guide: influence of sample sizes, position, and microwave power, *Food Bioprocess Technol.* (2010). <http://dx.doi.org/10.1007/s11947-009-0187-x>.
- [20] W. Klinbun, P. Rattanadecho, Numerical model of microwave driven convection in multi-layer porous pack bed using a rectangular waveguide (effects of layered configuration, layered thickness and frequency), *ASME J. Heat Transfer* (2012). <http://dx.doi.org/10.1115/1.4005254>.
- [21] D. Salvi, D. Boldor, G. Aita, C. Sabliov, COMSOL multiphysics model for continuous flow microwave heating of liquids, *J. Food Eng.* 104 (3) (2011) 422–429.
- [22] T. Yousefi, S. Mousavi, M. Saghir, B. Farahbakhsh, An investigation on the microwave heating of flowing water: a numerical study, *Int. J. Therm. Sci.* 71 (2013) 118–127.
- [23] W. Choi, S. Lee, C. Kim, S. Jun, A finite element method based flow and heat transfer model of continuous flow microwave and ohmic combination heating for particulate foods, *J. Food Eng.* 149 (2015) 159–170.
- [24] P. Rattanadecho, The theoretical and experimental investigation of microwave thawing of frozen layer using microwave oven (effects of layer configurations and layer thickness), *Int. J. Heat Mass Transfer* 47 (2004) 937–945.
- [25] R. Promas, P. Rattanadecho, W. Jindarat, Energy and exergy analyses in drying process of non-hygroscopic porous packed bed using a combined multi-feed microwave-convection air and continuous belt system (CMCB), *Int. Commun. Heat Mass Transfer* 39 (2012) 242–250.
- [26] S. Barringer, K. Ayappa, E. Davis, H. Davis, J. Gordon, Power absorption during microwave heating of emulsions and layered system, *J. Food Sci.* 60 (1995) 1132–1136.
- [27] C. Chan, Y. Chen, Role of length scales on microwave thawing dynamics in 2D cylinders, *Sep. Sci. Technol.* 37 (2002) 3407–3420.
- [28] V. Rajakovic, D. Skala, Separation of water-in-oil emulsions by freeze/thaw method and microwave radiation, *Sep. Purif. Technol.* 49 (2006) 192–196.
- [29] A. Nour, R. Yunus, Z. Jemaat, Study on demulsification of water-in-oil emulsions via microwave heating technology, *J. Appl. Sci.* 6 (9) (2006) 2060–2066.
- [30] R. Palou, R. Camacho, B. Chavez, A. Vallejo, D. Negrete, J. Castellanos, J. Karamath, J. Reyes, J. Aburto, Demulsification of heavy crude oil-in-water emulsions: a comparative study between microwave and thermal heating, *Fuel* 113 (2014) 407–414.
- [31] E. Binner, J. Robinson, S. Silvester, S. Kingman, E. Lester, Investigation into the mechanisms by which microwave heating enhances separation of water-in-oil emulsions, *Fuel* 116 (2014) 516–521.
- [32] G. Mur, Absorbing boundary conditions for the finite difference approximation of the time domain electromagnetic field equations, *IEEE Trans. Electromagn. Compat.* 23 (1981) 377–382.
- [33] S. Patankar, *Numerical Heat Transfer and Fluid Flow*, McGraw-Hill, New York, 1980.